END
DATE
FILMED
2-78
DDC

Columbia University
in the City of New York

A REVIEW OF THEORIES FOR THE

FLUID DYNAMIC EFFECTS OF ROUGHNESS

ON LAMINAR LUBRICATING FILMS

by

H. G. Elrod

December 1977

Lubrication Research Laboratory
School of Engineering and Applied Science
Department of Mechanical and Nuclear Engineering
Columbia University
in the City of New York

A REVIEW OF THEORIES FOR THE

FLUID DYNAMIC EFFECTS OF ROUGHNESS

ON LAMINAR LUBRICATING FILMS

by

H. G. Elrod

December 1977

ABSTRACT

This report contains a comprehensive survey of theoretical work on the fluid dynamic effects of roughness in lubrication.

Of necessity, much of the report deals with Reynolds roughness; that is, roughness which can be locally analyzed with Reynolds equation because the wavelength of the roughness is not too short. One-sided and two-sided striated roughnesses are considered. Statistical and multiple-scale treatments are discussed and intercompared. Finally, the effects of short-wavelength roughness (Stokes roughness) are treated, as well as the consequences of slip in highly rarefied situations.

Some new results for isotropic Reynolds roughness, for Stokes roughness, and for molecular slip are given preliminary exposure.

CONTENTS

A REVIEW OF THEORIES FOR THE

FLUID DYNAMIC EFFECTS OF ROUGHNESS

ON LAMINAR LUBRICATING FILMS

by

H.G. Elrod

I. Introduction:

The purpose of this paper is to summarize some theoretical results concerning the effects of surface roughness on laminar lubricating films. Old and new work are inter-related, in an attempt to show what is known, and what needs to be found out. For potential investigators, a considerable bibliography is appended.

Surface roughness may be deliberately created, as in grooved bearings, to promote a pumping effect. It may be the consequence of a fabrication process, such as drilling, broaching, grinding, lapping. Or it may be the consequence of scratches produced by debris. Obviously, then, striations will be associated with many forms of surface finish.

For present purposes, it suffices to observe that, quite typically, roughness amplitude excursions have associated elevation angles of 10°. Dependent on operating conditions, this amplitude may become a substantial fraction of the film thickness,h,with characteristics wavelengths ranging from $0(h) \rightarrow \infty$.

In terms of film-thickness reduction, the analyses to be discussed herein are to be regarded as the last purely fluid dynamical treatments before some solid-to-solid inter-

action of asperities takes place. The flow is treated as lam-
inar and Newtonian, with either liquid or gas, unless other-
wise specified. Cavitation or film rupture sometimes occurs
in conjunction with roughness, as in face seals. But these
effects are not examined here. On the other hand, molecular
slip, which takes place in ultra-thin gas passages, is dis-
cussed.
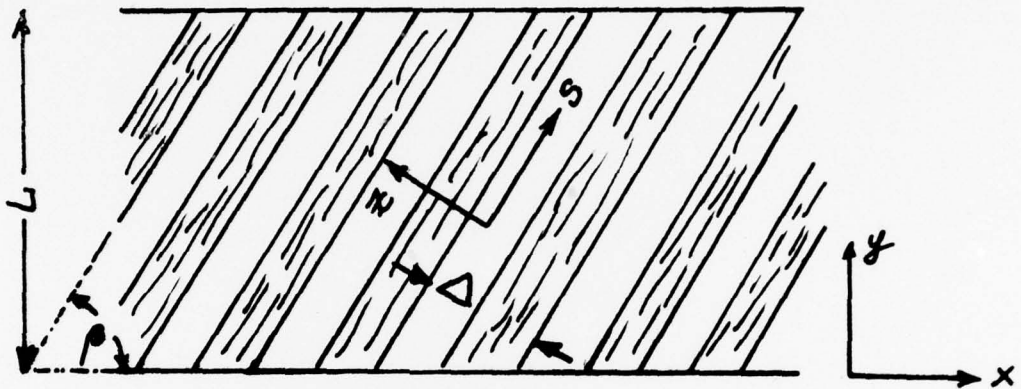
Figure 1.1 Striated Roughness

Figure 1.1 shows the striated roughness with which
this paper is mostly concerned. The film thickness is a
function only of the coordinate, z. Its cross-section may
be arbitrary, but is almost periodic. The moving surface is
smooth, and has, by choice of angle, "β", only an x-wise com-
ponent, U. When $\beta=\pi/2$, the striations are called "transverse",
and when $\beta=0$, the striations are "longitudinal".

If the characteristic wavelength, Δ, of the striations
is large compared with the gap, h, then it is legitimate to
use Reynolds equation to evaluate roughness effects. Such
roughness we term "Reynolds Roughness". On the other hand,
if the wavelength is so small as to necessitate the use of the
full Stokes equation, we use the name "Stokes Roughness".

II. Analysis of Discrete Rippling.

The earliest analyses of roughness effects were made by means of Reynolds equation for simple cross-sections si- nusoidal, rectangular, triangular). Michell (1) and Burton (4) used sinusoidal, first-order linearization treatments, the former with longitudinal striations on a simple slider bearing, and the latter with transverse striations in a par- allel-plate thrust situation. Such analyses are useful in disclosing some possible effects of roughness, but do not yield the load, which is a second-order effect.‡

Finite-difference solutions of Reynolds equation in the presence of roughness were obtained by Cameron (3)(trans- verse), Dowson & Whomes (7)(longitudinal), Shelly and Ettles (8)(longitudinal & transverse), and by Tønder & Christensen (9)(longitudinal). Because of the necessity of numerical description of individual grooves, it is not feasible to in- corporate in analyses of finite bearings a large number of striations. Thus the hypothesized surfaces, although retain- ing validity in their own right, are not realistic renditions of typical roughness profiles .... their roughness wavelength is too long. Nevertheless, some of these numerical studies show the important fact that the characteristic wavelength of the roughness ceases to affect Reynolds-equation solutions, even when it is only moderately small compared with overall bearing dimensions.

---

‡ Footnote: Although reference (1) is widely quoted as providing the effects on load due to longitudinal roughness, the small-roughness portion of the analysis actually just ex- hibits the effect of enlarged mean clearance.

$$B/A = 0.37.$$
* Points of inflection.
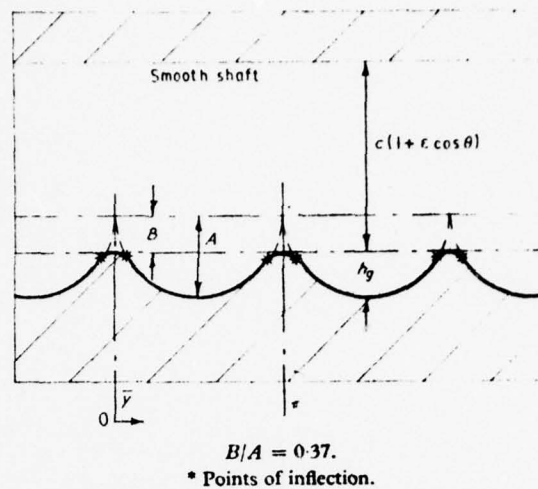
Figure 2.1   Assumed Waveform of
Machining Marks
(from ref. 2.8)

Figure 2.1 shows the profile assumed by Shelly and
Ettles to mimic machining marks from aero boring (longitudi-
nal) or from broaching (transverse). They studied the effects
on the performance of a 50.8 mm diam. journal bearing, 17.8 mm
long, with incompressible lubricant.

Figure 2.2 presents their results for a protuberance
amplitude (h_g) of 1.6 µm in a clearance (c) of 25.4 µm. The
roughness wavelength was varied to produce different numbers,
n, of waves either circumferentially (longitudinal) or axially
(transverse). Solutions include cavitation with Reynolds
boundary-condition ($p=\frac{dp}{d\theta}=0$). Note the dramatically rapid
approach of the load capacity to an asymptotic value. (The
indicated load reductions are the consequence of basing the
reference "smooth" loads on minimum, rather than mean, film
thickness). The early work of Cameron (3) with transverse
waves on an infinitely-wide slider (see Fig.2.2), and the more
recent work of Tønder and Christensen (9) with longitudial
waves on cylindrical rollers exhibit the same asymptotic effect.
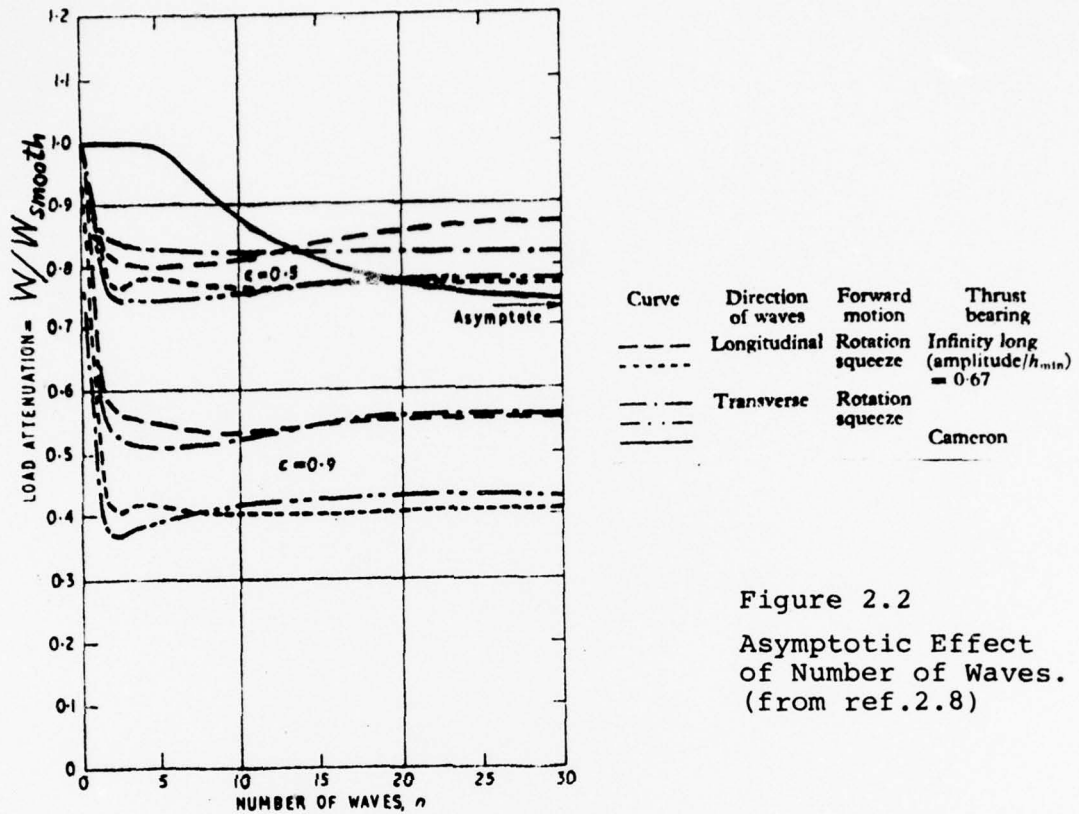
Figure 2.2

Asymptotic Effect
of Number of Waves.
(from ref.2.8)

For the special case of roughness in the form of rec-
tilinearly striated rectangular grooving, Reynolds equation
reduces to Laplace's eq., $\nabla^2 p = 0$,
in each of the constant film-thicknesses regions. Muijderman
(10) showed an exact solution could be obtained for the pres-
sure distribution by the juncture of linear patterns, (see
Fig. 2.3) all conditions being satisfied except for edge ef-
fects at the entrance & exit of the grooving. In the case
shown, there are pressure ripples across the grooving super-
imposed an a general buildup along the grooving. Subject to
the limitations of Reynolds equation and the hypothesis of in-
compressible Newtonian lubricant, the excursions of the pres-
sure ripple can be very substantial, and need only be small
compared with the total pressure buildup from the pumping ac-
tion, to minimize edge corrections.

Figure 2.3 Pressure Ripples Generated
Across Rectangular Roughness
Elements (from ref.10)

III. Averaged Variables with One-Sided Reynolds Roughness.*

Even with the deliberate roughness of herringbone and spiral-groove bearings, where Δ/L is much greater than for typical surface roughness, it is desirable, if possible, to deal with average pressures and average film thicknesses. On good authority, the writer has been told that an analysis achi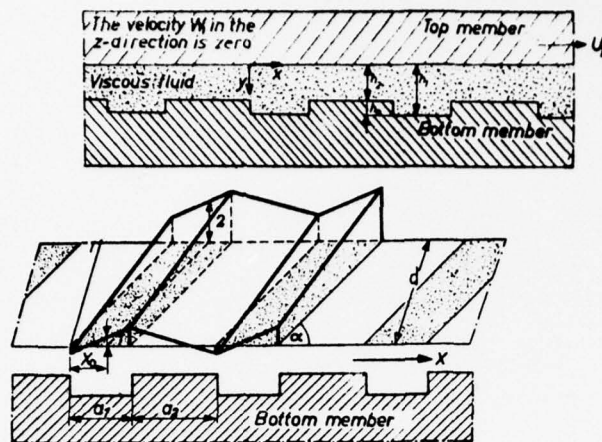eving this purpose was accomplished by Boeker circa 1944 (11a). However, the first publicly disseminated analysis is due to Whipple (11b).

The analysis of Whipple, as well as those of Muijderman (10), Hirs (12), and Elrod (13), takes advantage of the pressure periodicity associated with parallel opposing surfaces, with surfaces uniformly grooved. Whipple and Muijderman consider rectangular grooving only, whereas Hirs and Elrod account for "arbitrary" roughness. We summarize briefly here Hirs' analysis.

Figure 1.1 illustrates the situation analyzed. The smooth upper face (towards reader) moves with velocity U in the x-direction. Pressures at y=0 and y=L are uniform at p_0 and p_L, respectively. The bearing has infinite extent in the x-direction. Without proof, Hirs makes the following plausible statements for the narrow-groove limit (i.e., when $\Delta/L \ll 1$) with an incompressible fluid.

a) $\frac{\partial p}{\partial s}$ is independent of position (an hypothesis made earlier by Michell(2.1)

b) Q_z, the film flow in the z-direction, is independent of position.

---

* The roughness pattern must not move with respect to the gross mean-film configuration.

Applying Reynolds relations for the volumetric flows, one obtains from (a):

$$(Q_s)_m = - \frac{1}{12}(h^3)_m (\frac{\partial p}{\partial s})_m + \frac{1}{2}U(\cos\beta)(h)_m \qquad [3.1]$$

where the subscript "m" indicates an average over one wavelength, Δ, that includes one groove-ridge pair.

In addition, one obtains from (b):

$$(Q_z)_m \left\{ \frac{1}{(h^3)} \right\}_m = - \frac{1}{12\mu}(\frac{\partial p}{\partial z})_m - \frac{1}{2}U(\sin\beta)\left\{ \frac{1}{(h^2)} \right\}_m \qquad [3.2]$$

Since spatial differentiation and integration commute:

$$(\frac{\partial p}{\partial s})_m = (\frac{\partial \bar{p}}{\partial s})_m \quad , \quad (\frac{\partial p}{\partial z})_m = (\frac{\partial \bar{p}}{\partial z})_m \qquad [3.3]$$

where $\bar{p}$ is the local mean pressure. ‡ With Q_x and Q_s constant, both eqs. 3.1 & 3.2 can be integrated subject to pressure or flow boundary conditions. The performance of a simple herringbone bearing can thereby by computed.

Details have been given here because the same equations are crucial to the theory of Christensen (see section IV), and because it is feasible, even in a review paper, to do so. We shall reserve comment on the assumptions (a) and (b) until section V.

In ref, (13) the same problem is attacked by assuming that the pressure can be expanded in terms of $\eta \equiv y/L$ and $\zeta = z/\Lambda$ with $\epsilon \equiv \Delta/L$ as a small parameter. Thus:

---

‡ Strictly, the $\bar{p}$'s for the s- and z derivatives are not the same except for linear pressure profiles, but the discrepancy vanishes as $\Delta/L \rightarrow 0$.

$$p = p_0(\eta,\zeta) + \varepsilon p_1(\eta,\zeta) + \varepsilon^2 p_2(\eta,\zeta) \text{ etc.} \qquad [3.4]$$

This expansion is used in connection with

$$h = h_0 + \varepsilon f(\zeta) \qquad [3.5]$$

and Reynolds equation, and periodicity is invoked. Differential equations are found for p_0, the mean pressure, p_1, the first order pressure ripple, etc. The results apply for incompressible and compressible lubricants, and, in a sense, legitimize earlier, more intuitive work.

The limitation of constant mean film thickness, embodied in Whipple's work, was removed by Vohr and Pan (14), again on an intuitive basis. Their formulations are for the rectangular-grooving equivalents of eqs. (3.1) and (3.2). These expressions they employ with local mean thicknesses and local mean fluid density, $\bar{\rho}$, and write:

$$\nabla \cdot \bar{\rho}\vec{Q} = 0 \qquad [3.6]$$

Many useful studies of grooved-bearing performance have been made employing the Vohr-Pan differential equation.

In ref. (15) a small-parameter, multiple-scale analysis is used to generate the appropriate differential equations for varying mean film thickness, arbitrary orientation of the roughness striations, and arbitrary roughness cross-section. The expansion adopted is:

$$p = p_0(\eta,z,\zeta) + \varepsilon p_1(\eta,z,\zeta) + \varepsilon^2 p_2(\eta,z,\zeta) \text{ etc.} \qquad [3.7]$$

explicit recognition being given to the possible of slow pressure variation in terms of the "slow" variable, z, and fast

variation (rippling) in terms of the "fast" variable, ζ. An analogy might be the expression of atmospheric temperature in in terms of month and hour of the day. The slow seasonal temperature trend would be known as a function of the month, and the daily fluctuation as a function of the hour. Again, the analysis is in agreement with more heuristic formulations; namely, eq.(3.6) with components of $\vec{Q}$ given by eqs. (3.1) and (3.3) is supported.

Within their stated regions of validity, all of the foregoing (section III) analyses yield results identical to those to be given in the next section.

IV. Statistical Treatments of One-Sided Reynolds Roughness.

The haphazard, semi-random distribution of roughness on many surfaces has lead investigators to consider statistical methods of analysis. The first such treatment was made by Tzeng & Saibel (16). Figure (4.1) shows the system
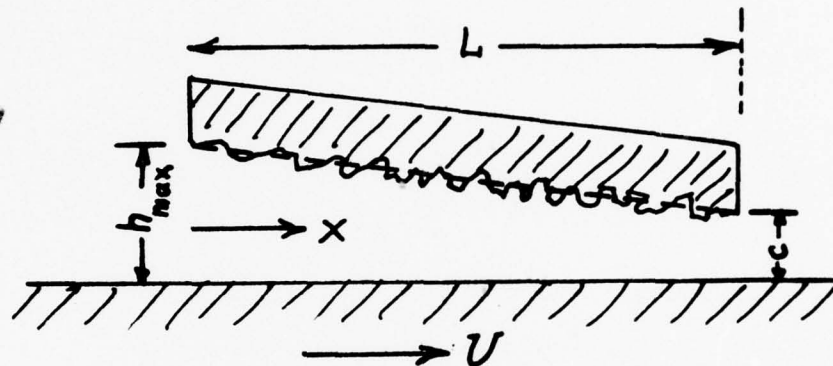
Figure 4.1   Simple Slider Bearing with Roughness on One Surface

analyzed.‡   The authors write, for an incompressible fluid:

$$\frac{d}{dx}h^3\frac{dp}{dx} = 6\mu U\frac{dh}{dx} \qquad [4.1]$$

where "h" is the film thickness <u>including</u> roughness. One integration yields:

---

‡ Fig. 1 of ref.(16) shows two-sided roughness, for which their analysis is not applicable because of the neglect of time-derivatives. (See section VI) The same comment applies to refs. (18,19,20).

$$\frac{dp}{dx} = \frac{6\mu U}{h^2} - \frac{12\mu Q}{h^3} \qquad\qquad [4.2]$$

Now the authors write:

$$h = \bar{h}(x)+\theta \qquad\qquad [4.3]$$

where $\bar{h}$ is the mean of a population of bearings with similar nominal specification and "θ" is some random fluctuation about the mean, being different from bearing to bearing.

Thus: $<h>$ (expected value) $= <\bar{h}+\theta> = \bar{h}$ [4.4]

The authors now <u>hypothesize</u> that the through-flow, Q, will be similar for all bearings of this type, and take the expected values of the quantities in eq.(4.2). The result is:

$$<\frac{dp}{dx}> = \frac{d<p>}{dx} = 6\mu U<\frac{1}{h^2}> - 12\mu Q<\frac{1}{h^3}> \qquad [4.5]$$

The boundary conditions on $<p>$ are:

$$<p(0)> = <p(L)> = 0$$

Integration of eq.(4.5) yields the load.

Thus:

$$\text{Load} = \int_0^L <p>dx \qquad\qquad [4.6]$$

To use these equations, some knowledge of the roughness distribution is necessary. Tzeng & Saibel proposed a so-called "beta distribution" function which yields finite maximum deviations from a mean asperity height, but other-

wise closely resembles a Gaussian normal distribution. Christensen(18) followed their example with a slightly different expression, which to avoid confusion, is the only one to be given here:

$$f(\theta) = \frac{35}{32c}\left\{1-\left(\frac{\theta}{c}\right)^2\right\}^3; \quad -c<\theta<c \qquad [4,7]$$

According to this formula, the fraction of asperities at a given "x" in the bearing population with heights (measured from a mean) between h_{s1} and h_{s2} is:

$$\int_{h_{s2}}^{h_{s1}} f(\theta)d\theta$$

The function is compared with the normal distribution curve in Fig.(4.2)
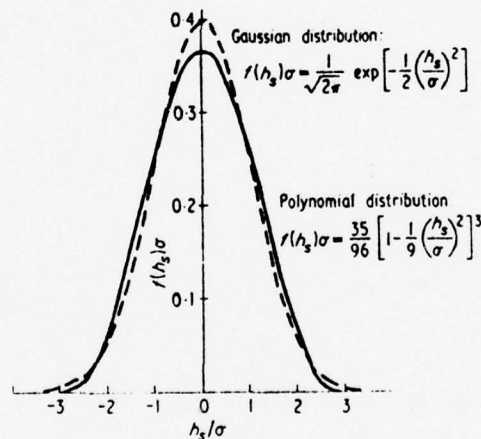
Figure 4.2   Roughness Distribution
            Curves Compared
            (from ref.18)

Note that the maximum amplitude is three standard deviations (i.e., c=3σ).

Tzeng & Saibel cite only one numerical example, but their analysis yields the curves for transverse roughness shown in Fig.4.3.
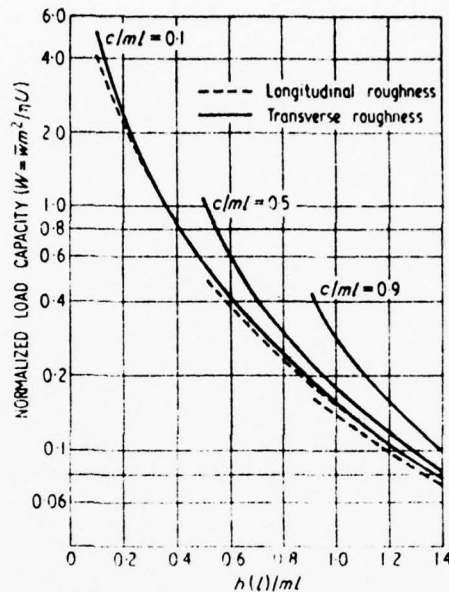
Figure 4.3   Effect of Roughness on
             Load Capacity of Infinitely
             Wide Slider Bearing
             (from ref.18)

Christensen(18) and Christensen & Tonder(9,19,20) adopt a somewhat different statistical viewpoint. They regard the function $f(\theta)$ as providing the roughness distribution for the population of surface elements neighboring a given "x" in a given bearing. This difference in approach has lead to misunderstanding, even among the analysts themselves(18).

Essentially, the Christensen (18) roughness theory rests on the same two postulates adopted by Hirs (12), but with the Vohr-Pan (14) viewpoint that the flow relations (3.1) and (3.2) are locally applicable in a bearing with variable

mean film thickness. In addition, accenting the uncertainty of the actual roughness distribution, they interpret all means as statistical expectations.

For transverse roughness, $\theta=\theta(x,t)$ or $\beta=\pi/2$, eqs.(3.1), (3.2), and

$$\nabla \cdot \vec{Q} = \frac{\partial \bar{h}}{\partial t} \qquad [4.8]$$

leads to one of Christensen's differential equations:

$$\frac{\partial}{\partial x} \frac{1}{\overline{h^{-3}}} \frac{\partial \bar{p}}{\partial x} + \frac{\partial}{\partial y} \overline{h^3} \frac{\partial \bar{p}}{\partial y} = 6\mu U \frac{\partial}{\partial x} \frac{\overline{h^{-2}}}{\overline{h^{-3}}} + 12\mu \frac{\partial \bar{h}}{\partial t} \qquad [4.9]$$

For longitudinal roughness, $\theta=\theta(y,t)$ or $\beta = 0$, his result is: ∗

$$\frac{\partial}{\partial x} \overline{h^3} \frac{\partial \bar{p}}{\partial x} + \frac{\partial}{\partial y} \frac{1}{\overline{h^{-3}}} \frac{\partial \bar{p}}{\partial y} = 6\mu U \frac{\partial \bar{h}}{\partial x} + 12\mu \frac{\partial \bar{h}}{\partial t} \qquad [4.10]$$

Here $\overline{h^n}$ stands for the local mean value or expectation of h^n.

In addition, for uniform isotropic roughness with steady-state operation, Christensen & Tønder propose (19,20):

$$\frac{\partial}{\partial x} \overline{h^3} \frac{\partial \bar{p}}{\partial x} + \frac{\partial}{\partial y} \overline{h^3} \frac{\partial p}{\partial y} = 6\mu U \frac{\partial \bar{h}}{\partial x} \qquad [4.11]$$

These differential equations resemble very closely the usual Reynolds equation, although, as Christensen points, there is no completely equivalent smooth bearing to be found by adopting some appropriately chosen mean film thickness. But the numerical treatments are almost identical ...... and there is no necessity, either, of treating every little ripple individually.

∗ The more general case of arbitrary striation angle, β, and variable fluid density is treated in (15).

Christensen and Tønder have applied differential equations (4.9) and (4.10) to slider and journal bearings of finite and infinite width (18,19,20) using roughness distribution function (4.7). Fig.(4.3) shows the theoretical load capacities of the slider bearing in Fig. (4.1) for the two types of roughness, longitudinal and transverse. It is seen that the longitudinal roughness has scarcely any influence on load, whereas the transverse roughness certainly can produce a measurable increase in load capacity over that for a perfectly smooth bearing. Notice that the curves terminate where c/mL=h/mL since there is then incipient contact of the asperities with the smooth opposing surface.

The effect of transverse roughness on slider friction is shown in Figures (4.4) and (4.5).
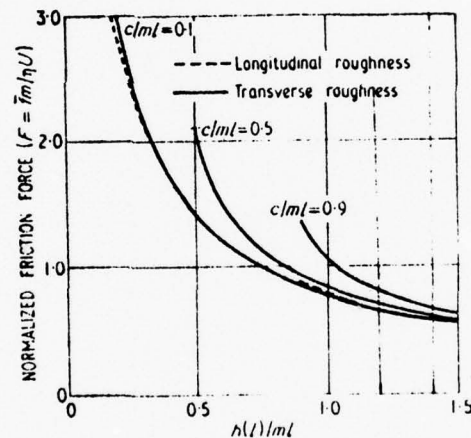
Figure 4.4 Longitudinal and Transverse Roughness Effects on Slider Friction. (from ref.16).

From Fig. (4.4) it is observed that longitudinal roughness scarcely affects the friction at all, whereas transverse roughness can increase it appreciably. However, for a given
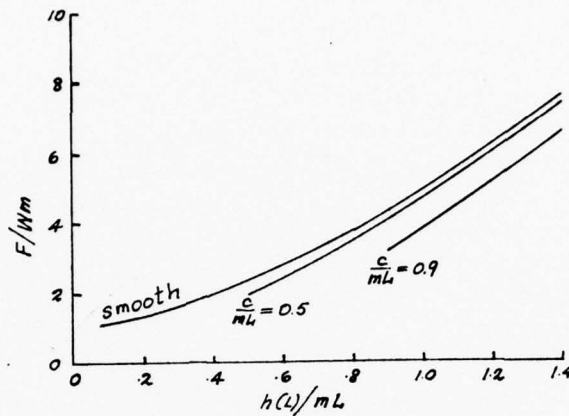
Figure 4.5 Normalized Friction
Coefficient (C_f/m) with
Transverse Roughness
(adapted from (16)).

mean film thickness, the friction coefficient is reduced by
transverse roughness, as shown in Fig. (4.5).

Christensen (18) summarizes his findings in the table
below.

COMPARISON OF SURFACE ROUGHNESS EFFECTS

Bearing characteristic	Longitudinal roughness	Transverse roughness
Load capacity	Small decrease	Significant incr.
Oil flow	Small increase	Significant decr.
Friction force	Insignificant increase	Significant incr.
Friction coefficient	Significant increase	Significant decr.
Temperature rise	Insignificant increase	Highly significant incr.

V. Intercomparison of Theoretical Methods

This is perhaps an appropriate place to summarize some of the different viewpoints embodied in the analyses of Sections II, III and IV, and to make intercomparisons.

In Section II the common feature is the assumption of some specific roughness contour (rectangular, sinusoidal, etc.) to which Reynolds equation is applied, either by a small-perturbation analysis or by a direct numerical method. Moreover, the detailed interaction between the surface roughness and the lubricating film is followed.

In Section III, on grounds of periodicity or short roughness wavelength, detailed interactions are "smeared" or averaged, and differential equations are developed which permit calcualtions of load capacity, friction and other pertinent bearing quantities for wide classes of bearing configurations.

In Section IV, two different statistical approaches are used to derive differential equations for bearing performance. The second of these approaches has now been quite extensively applied.

We have already seen that there is a high degree of overlap in applicability between the most general of the developments described in Section II (ref.15) and the most general development in Section III (ref.18) (with the latter having publication priority). We have also seen that, for roughness wavelengths which are small compared with overall bearing dimensions, the results of Section I are in accord with those of II and III, when the particular form of roughness is taken into consideration. The question may now be asked: "To what extent does the particular form of roughness matter"?

For small-amplitude roughness, the answer is given in refs. (13) and (18), where it is shown that, in this case, the special character of the roughness does not matter, only its rms value. Consider the differential equations (4.9) and (4.10). Four means of the film thickness appear namely,

$$\overline{h^3} \ , \ \overline{h^{-3}} \ , \ \overline{h^{-2}}/\overline{h^{-3}} \text{ and } \bar{h}$$

The values for these quantities which would arise for the same specified $\bar{h}$ and variance, σ, are now in question.

If all roughness shapes resulted in exactly the same values for the first three of these quantities, identical pressure distributions would be predicted.

Now the first quantity, $\overline{h^3} = \overline{(\bar{h}+\theta)^3} = \bar{h}^3 + 3\sigma^2$

is the same for <u>any</u> symmetrical roughness distribution. Results for the other quantities, $\overline{h^{-3}}$ and $\overline{h^{-2}}/\overline{h^{-3}}$ are compared in Figs. (5.1) and (5.2) for simple sinusoidal and rectangular roughness, and for the roughness distribution adopted by Tzeng & Saibel and Christensen & Tønder eq.(4.1). Even when $\sigma/h=0.2$ (0.33 corresponds to incipient solid-solid contact), the discrepancies for $\bar{h}^3 \ \overline{h^{-3}}$ and for $\overline{h^{-2}}/\bar{h} \ \overline{h^{-3}}$ do not exceed 4%. Therefore, in so far as Reynold roughness analyses are concerned, there is virtually nothing to choose among the different forms.

In Section IV, the difference between the Tzeng & Saibel and Christensen & Tønder statistical approaches was defined. Why, then, do the authors use virtually the same asperity distribution function? Because, as a practical matter the bearing population concept (many "like" bearings) is difficult to implement, not only because of the number of
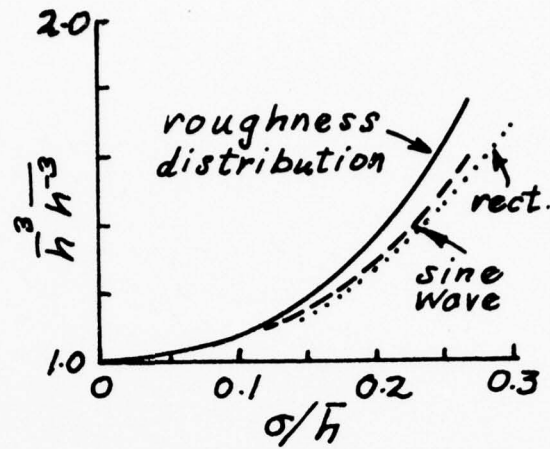
Figure 5.1   Comparison of Diffusive
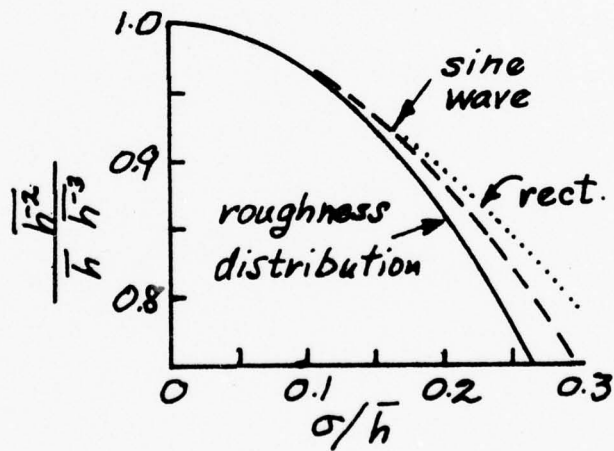Roughness Parameters.

Figure 5.2.   Comparison of Convective
Roughness Parameters.

bearings required, but because of the virtual impossibility of ascertaining positions "x" within the film to accuracies of the order of roughness wavelength. These considerations do not, of course, invalidate the Tzeng & Saibel approach, nor their slider analysis. In actuality, though, Tzeng & Saibel must invoke an "ergodic hypothesis", namely that the spatial distribution of asperities on a given bearing is similar to that obtained from replication of the bearing sample. This reconciliation of roughness distributions does not, however, render the difference in the two statistical approaches trivial, since the local sampling approach of Christensen & Tønder permits them to generate second-order partial differential equations applicable to a wide variety of bearings.

In a manner of speaking, the analyses of Section II embody microscopic determinism, those of Section III embody macroscopic determinism, and those of Section IV embody macroscopic statistical analysis. It is indeed reassuring to see the agreement achieved, and there is always merit in "seeing a problem from different viewpoints. However, we have so far considered only one-sided roughness, and some questions need to be answered before more difficult problems can be successfully tackled. For example, most of the macroscopic deterministic analyses (refs.11-14) take advantage of periodicity or quasi-periodity (high spatial correlation) to derive load support relations, whereas the statistical analysis of ref. (18) invokes randomness (low correlation). Yet both approaches yield the same results!

The answer to this paradox lies in the fact that statistical analyses of Reynolds equation have depended on the two postulates leading to eqs. (3.1) and (3.2), generalized,

however, to allow for weak spatial dependence.‡   But once
these postulates are accepted, there is really little need
for statistics! For example, generalizations of the mass-
flux relations (3.1) and (3.2) then follow, whether or not
the striations are random. It is undeniably desirable to be
aware of the likely response of a film to haphazard surface
fluctuations but, it is also desirable to separate the cru-
cial from the non-crucial arguments in a derivation.

Since the validity of the Reynolds roughness equations
hinges on the correctness of the mass-flux postulates,one may
legitimately ask when they are valid. As Christensen (18)
emphasizes, and as all investigators agree, ... in the
limit of short roughness wavelength. This conclusion is man-
ifest by the numerical studies cited in Section II, and sup-
ported by the multiple-scale analysis in (15). However, if
these postulates are taken as the starting point for a rough-
ness analysis, all trace of wavelength disappears from the
equations! So there can be no self-checking for consistency.
Nevertheless, these postulates have physical relevance and
irresistible simplicity, so all of us will doubtless continue
to use them in new applications, confident that experiment
and further mathematics will later corroborate.

Mathematically, the point to be made concerning the
postulates is that they constitute guesses concerning solu-
tions of Reynold equation. If one is to use Reynolds equa-
tion, why not use it from start to finish?   The multiple-
scale analyses in refs. (15,21) essentially accomplish this
objective for one-sided roughness. The series in $\Delta/L=\epsilon$ of
eq. (3.1) is carried through to second-order, and interior

---

‡ The analysis of Tzeng & Saibel (16) postulates
that the total bearing throughput, Q, will be invariant.

solutions (to eqs. like (4.9) and (4.10)) are asymptotically
matched at film peripheries by Muijderman-type boundary so-
lutions (22). Additional aspects of film shape manifest
themselves in the second-order treatment, with rectangular
grooving preserving striking simplicity. The internal con-
sistency of the whole treatment is very convincing, but the
analytical difficulty is such as to discourage immediate
attempts on more complicated roughness patterns (two-sided,
two-dimensional, etc.).

While difficulties have been pointed out in the deri-
vation by statistics of differential equations for Reynolds-
type roughness, there can be no doubt that statistics are
often necessary to describe properties of the roughness it-
self. In order words, the coefficients in differential equa-
tion such as (4.9) and (4.10) indicate what properties of
the local film contour are required, and statistical distri-
bution functions such as (4.7) give our best estimate of
their values.

On the other hand, it is writer's opinion that, at the
present time, much can be still be learned by using simple
roughness functions and the short-wavelength postulates.
Statistics should be used sparingly, and principally to pro-
vide numerical estimates of various roughness parameters.

A conceptual difficulty which the smoothening and statis-
tical approaches have in common is the definition of sample
space for local averages. Both suppose the existence of
such local averages to be not critically dependent on the
choice of sample size. The problem here is precisely the same
as the definition of density for a gas. For too small a sam-
ple volume, fluctuations in the value of density occur as
individual molecules are included or excluded from the volume.
For too large a sample space, density definition is lost en-
tirely and a simple average for all available space results.

VI. Two-Sided Reynolds Roughness

In 1971 Berthe & Godet (23) pointed out that roughness analyses up to that time were not appropriate for films with two rough bounding surfaces if mutual tangential motion should also be present. Let us now consider situations where
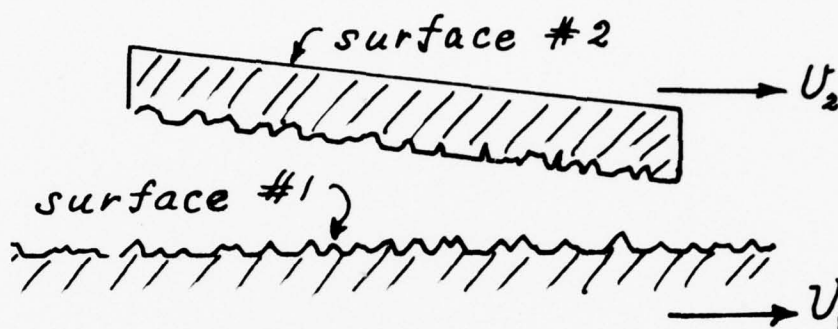
Figure 6.1   Two Rough Moving
Surfaces.

such surfaces are involved. In these instances, the roughness on the moving surface "sees" a varying mean film thickness. For example, in Figure 6.1, surface #1 is "moving" if $U_1 \neq U_2$. A steady-state case with transverse roughness will be treated. The film-thickness distribution is given by:

$$h = \bar{h}(x) + \theta_1(x-U_1t) + \theta_2(x-U_2t) \qquad [6.1]$$

and the applicable Reynolds equation for an incompressible fluid is:

$$\frac{\partial}{\partial x} \frac{h^3}{12\mu} \frac{\partial p}{\partial x} + \frac{\partial}{\partial y} \frac{h^3}{12\mu} \frac{\partial p}{\partial y} = \frac{(U_1+U_2)}{2} \frac{\partial h}{\partial x} + \frac{\partial h}{\partial t} \qquad * \qquad [6.2]$$

---

* Velocities are restricted to the x-direction

Substitution of the film-thickness expression (6.1) into (6.2) yields:

$$\frac{\partial}{\partial x}\left\{\frac{h^3}{12\mu}\frac{\partial p}{\partial x} - \frac{(U_1+U_2)}{2}\bar{h} + \frac{(U_1-U_2)}{2}(\theta_1-\theta_2)\right\} + \frac{\partial}{\partial y}\frac{h^3}{12\mu}\frac{\partial p}{\partial y} = 0 \qquad [6.3]$$

For the case of two-dimensional contact of cylinders in pure rolling, $U_1=U_2=U$ and $\partial/\partial y=0$, and eq.(6.3) reduces to:

$$\frac{\partial}{\partial x}\frac{h^3}{12\mu}\frac{\partial p}{\partial x} = U\frac{\partial\bar{h}}{\partial x} \qquad [6.4]$$

This equation can be explicitly integrated subject to boundary conditions on "p". Michau, Lafont, Berthe and Godet (24) and Tallian (25) have used it it estimate the pressures and pressure excursions due to rippling which may occur in rolling contact.

When $U_1{\neq}U_2$, rippling effects remain in the convective term of Reynolds equation. Thus for the simple, infinitely wide slider in Fig. 6.1, with $U_2=0$, eq. (6.3) becomes:

$$\frac{\partial}{\partial x}\left\{\frac{h^3}{12\mu}\frac{\partial p}{\partial x} - \frac{U_1}{2}\bar{h} + \frac{U_1}{2}(\theta_1-\theta_2)\right\} = 0 \qquad [6.5]$$

Chow and Cheng (26) invoke a generalized form of the flux continuity postulate, hypothesizing

$$Q_x = \frac{h^3}{12\mu}\frac{\partial p}{\partial x} - \frac{U}{2}(\bar{h}-\theta_1+\theta_2) \qquad [6.6]$$

as locally smooth and continuous. Precisely as in eq. (3.2), one then obtains:

$$Q_x\left(\frac{1}{h^3}\right)_m = -\frac{1}{12\mu}\left(\frac{\partial p}{\partial x}\right)_m - \frac{U}{2}\left\{\bar{h}\left(\frac{1}{h^3}\right)_m + \left(\frac{\theta_2}{h^3}\right)_m - \left(\frac{\theta_1}{h^3}\right)_m\right\} [6.7]$$

With Q_x taken as independent of "x", Chow & Cheng eliminate it by differentiation to obtain a second-order differential equation. This they apply to the elastohydrodynamic contact problem. Other forms of differential equation are derived by them for longitudinal roughness, and for different combinations of U_1, U_2.

The Chow-Cheng differential equations, although derived in a different manner (i.e., on a postulatory basis), are special cases of the differential equation published in ref. (27). This earlier derivation was via multiple-scales, and again in the interest of brevity, we shall forgo an account of the method. It is recommended, however, to those who would like to contribute new results in this field. The final result in (27) is:[*]

$$\frac{\partial}{\partial \tau}(\bar{H}\pi_0) + (\vec{\Lambda}_1+\vec{\Lambda}_2)\cdot\nabla(\bar{H}\pi_0) + \frac{\partial}{\partial n}[(\vec{\Lambda}_1-\vec{\Lambda}_2)\cdot\hat{n}\left\{\frac{I_2}{\overline{H^{-3}}} - \frac{I_1}{\overline{H^{-3}}}\right\}\pi_0] \; =$$

$$= \frac{\partial}{\partial s}(\overline{H^3}\pi_0\frac{\partial\pi_0}{\partial s}) + \frac{\partial}{\partial n}(\frac{1}{\overline{H^{-3}}}\pi_0\frac{\partial\pi_0}{\partial n}) \qquad\qquad [6.8]$$

Here the coordinate system consists of "n" normal to the striations ($\hat{n}$, the unit normal) and "s" parallel to the striations. The striations on one surface must be parallel to those on the opposing surface, but the fluid may be compressible ($\pi_0=1$ in all coefficients, if incompressible), "β" may be arbitrary, and the flow may be transient. In most instances, $I_1 = (\frac{\theta_1}{h^3})_m$ and $I_2(\frac{\theta_2}{h^3})_m$, as in eq. (6.7).

---

[*] "n" and "s" are here made non-dimensional with "L".

For the case of transverse roughness with a simple slider bearing, the effects of location of the roughness are shown in Fig. 6.2.
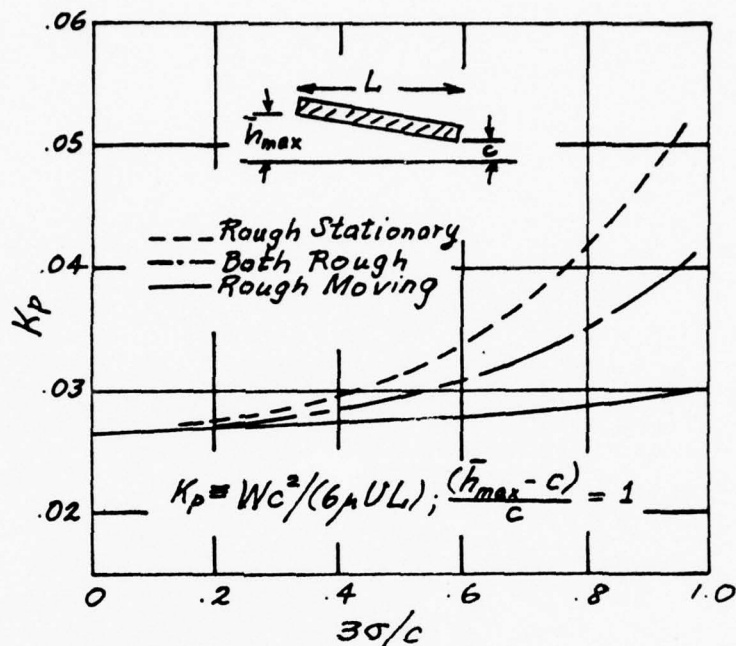
Figure 6.2 Load Capacity as Function of Transverse Roughness Location (from ref.27)

The maximum film thickness excursion due to roughness is the same for each curve, whether from one surface alone, or two in combination. The manner in which load capacity varies with location can be rationalized. Essentially, pressure buildup is the result of fluid resistance to being drawn by convective shear into a narrowing film. For given surface speed and mean film thickness, less resistance will be experienced if some of the fluid is drawn along in the interstices of a moving rough surface. Hence the lowest load capacity is associated with the "rough moving" curve of Fig. 6.2, with intermediate and highest capacities resulting from transfer of part, or all, of the roughness to the stationary surface.

The argument advanced above would lead one to conjecture that roughness would have less effect with a compressible fluid, since then the fluid "has the choice" of leaving a location by pressure gradient, or simple being compressed within the roughness depressions. Some examples in ref. (28) illustrate the phenomenon.

VII. Two-Dimensional Reynolds Roughness.

The next logical generalization of treatment is to non-striated, or two-dimensional Reynolds roughness. Naturally, as we advance in difficulty the applicable literature thins out.

For isotropic Reynolds roughness, Christensen & Tønder propose (see also eq.4.11)

$$\frac{\partial}{\partial x} \; \overline{h^3} \; \frac{\partial \bar{p}}{\partial x} + \frac{\partial}{\partial y} \; \overline{h^3} \; \frac{\partial p}{\partial y} = 6\mu U \frac{\partial \bar{h}}{\partial x} \qquad\qquad 7.1$$

To this writer's knowledge, no proof of this relation has appeared in the open literature. For reasons to be given below, I believe it to be incorrect.

There appears to be the opportunity for further progress along the lines of Hamilton, Walowit and Allen (29) and Tsao and Tong (30). These investigators determine by Reynolds equation the flow about a single cylindrical asperity with flat or spherically-capped top (Fig. 7.1).
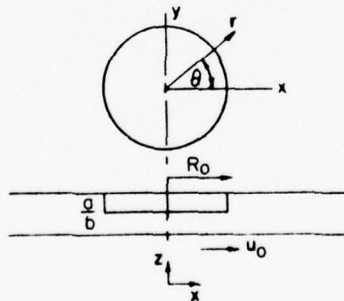
Figure 7.1   Asperity Geometry
(from ref. 29)

To mimic surface roughness, they then form a grid of such asperities (Fig. 7.2).
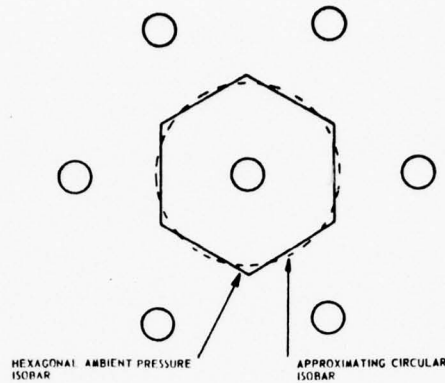
Figure 7.2.   Asperity Distributions
(from ref. 29)

An externally-impressed pressure gradient is not included in their analyses, their interest being chiefly in face seals. Cavitation is included, but only in the Gumbel sense with "lopping off" of negative pressures.

For a single asperity of the form shown in Fig. 6.1, where the film thickness has two different constant values, Reynolds equation reduces to Laplace's equation

$$\nabla^2 p = 0 \qquad\qquad\qquad [7.2]$$

in both inner ($r<R_0$) and outer ($r>R_0$) regions.   Suitable solutions are:

<u>Inner</u>: $p = k_1^i \, r$

$$\left. \right\} \; [7.3]$$

Outer: $p = k_1^c \, r + k_2^c/r$

Matching mass fluxes and pressures at the regional interface ($r=R_0$), we obtain:

Inner: $p = k_1^e x + Kx$

$\left.\right\}$ [7.4]

Outer: $p = k_1^e x + Kx(\dfrac{R_0}{r})^2$

where: $K = \dfrac{k_1^e\{(a+b)^3 - b^3\} - 6\mu Ua}{(a+b)^3 + b^3}$ [7.5]

The above pressure distributions consist of an externally-impressed gradient k_1^e, and a deviational component. Typical results for the latter are shown in Fig. 7.3.
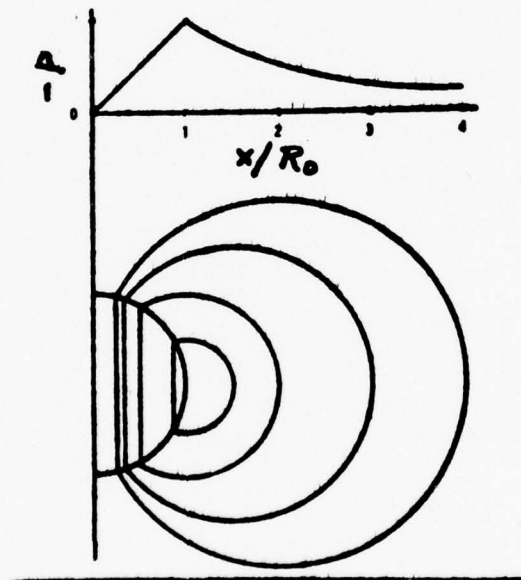
Figure 7.3. Typical Deviational Pressure Distribution ($\theta = 0$) and Isobars for Single Asperity (from ref.29)

Now although the disturbance (deviational) pressure vanishes at $r \rightarrow \infty$, there remains a net "drag" resulting from the asperity. Thus, limit $M \rightarrow \infty$.

$$\text{Drag} = \left[\int_{-M}^{+M} p\,dy\right]_{x=-L} - \left[\int_{-M}^{+M} p\,dy\right]_{x=+L} - \int_{-M}^{+M}(k_1^e 2L)\,dy \qquad [7.6]$$

The result, independent of $L > R_0$, is:

$$\text{Drag} = (\pi R_0^2) \frac{[12\mu Ua - 2k_1^e\{(a+b)^3 - b^3\}]}{(a+b)^3 + b^3} \qquad [7.7]$$

No net disturbance effect exists for the flow.

Now if many protuberances were present on a surface, as a first approximation one might consider each immersed in an external pressure gradient, partly impressed by outside agencies and partly an integrated effect from other asperities. A macroscopic theory relating average flow to surface velocity and average pressure gradient might thereby be built. This analysis has yet to be done.

For the case of purely Poiseuille flow ($U_1 = U_2 = 0$) a satisfactory analysis can be made. The differential equation is:

$$\frac{\partial}{\partial x} h^3 \frac{\partial p}{\partial x} + \frac{\partial}{\partial y} h^3 \frac{\partial p}{\partial y} = 0 \qquad [7.8]$$

This is the heat conduction equation with "p" playing the rôle of temperature, "h^3" playing the rôle of thermal conductivity and lineal mass flow playing the rôle of heat flux.

In ref.(31) it is proved that the heat flow through a region will be less than that with arbitrarily assumed shapes for the isotherms, and greater than that with arbitrarily assumed lines of heat flow (adiabats). Translated to Reynolds equation, this statement becomes: the lineal mass flow will be less than with arbitrarily assumed isobars and greater than that with arbitrarily assumed streamlines. Let us apply this theorem to the roughness pattern shown in Figure (7.4).
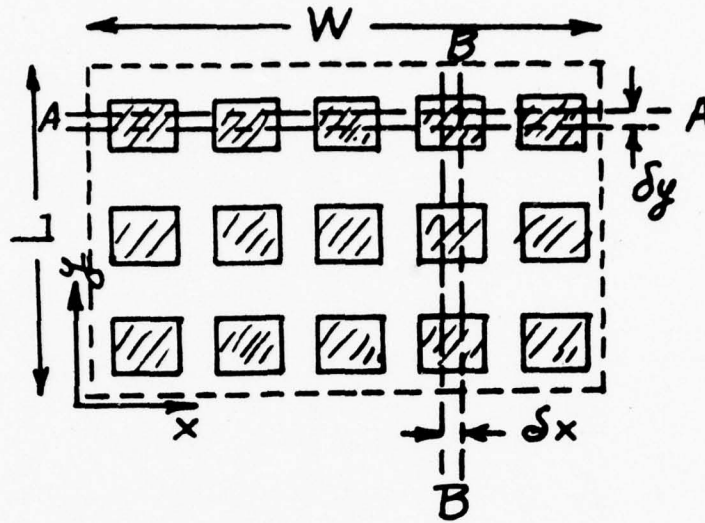
Figure 7.4   Two-Dimensional Roughness
Pattern

First, assume that the isobars are horizontal. Then for the
strip "δy" lying along A-A, "δp" must be constant. The local
mass flow is

$$(\dot{m}_y \delta y) = \frac{-h^3}{12\mu}\delta p \qquad\qquad [7.9]$$

The integrated mass flow along the stretch "W" is:

$$(\delta y)\dot{M}_y = -\frac{1}{12\mu}\int_0^W h^3 dx\,\delta p \equiv -\frac{W}{12\mu}\overline{h^3}^x \delta p \qquad [7.10]$$

Or: $$dp = -\frac{12\mu\dot{M}_y}{W}\frac{dy}{\overline{h^3}^x} \qquad\qquad [7.11]$$

A second integration, this time with respect to "y",
yields:

$$p(L)-p(0) = -\frac{12\mu\dot{M}_y}{W}\int_0^L \frac{dy}{h^3 x} \equiv -\frac{12\mu\dot{M}_y}{W}\overline{\left(\frac{1}{h^3 x}\right)}^y L \qquad [7.12]$$

Now so long as "W" and "L" contain many roughness elements, eq. (7.12) is, effectively:

$$(\dot{m}_y)_m = -\frac{1}{12\mu}\left[\overline{\left(\frac{1}{h^3 x}\right)}^y\right]^{-1}\frac{\partial \bar{p}}{\partial y} \qquad [7.13]$$

and this is an upper limit for the flow.

Alternatively, one can assume vertical streamlines, such as those for "δx" between B-B in Figure (7.4). In this case, for each element "δx":

$$(\dot{m}_y)h^{-3} = -\frac{1}{12\mu}\frac{\partial p}{\partial y} \qquad [7.14]$$

$$p(L)-p(0) = -12\mu(\dot{m}_y)\int_0^L h^{-3}dy \equiv -12\mu\dot{m}_y\overline{h^{-3}}^y L \qquad [7.15]$$

With the gross pressure difference p(L)-p(0) treated as constant, integration is now performed along "W" to give:

$$\dot{M}_y = -\frac{1}{12\mu}\frac{p(L)-p(0)}{L}\int_0^W \left\{\overline{h^{-3}}^y\right\}^{-1}dx$$

$$\equiv -\frac{1}{12\mu}\frac{p(L)-p(0)}{L}\overline{\left(\frac{1}{h^{-3}y}\right)}^x W \qquad [7.16]$$

A lower limit for the flow is thus obtained:

$$(\dot{m}_y)_m = -\frac{1}{12\mu}\overline{\left(\frac{1}{h^{-3}y}\right)}^x \frac{\partial \bar{p}}{\partial y} \qquad [7.17]$$

Potential error in the estimate for $(\dot{m}_y)_m$ is minimized by use of the arithmetic average from eqs. (7.13) and (7.17) Thus:

$$(\dot{m}_y)_m = \frac{1}{24\mu}\left[\left(\overline{\frac{1}{h^{-3}}}^y\right)^x + \left\{\left(\overline{\frac{1}{h^3}}^x\right)^y\right\}^{-1}\right]\frac{\partial\bar{p}}{\partial y} \qquad [7.18]$$

For the case of heat conduction and a configuration similar to that shown in Fig.(7.4), Yovanovich(32) has found the error of the equivalent of eq. (7.18) not to exceed 5%. For isotropic roughness the indicated averaging processes must be independent of direction. Equation (7.18) then reduces to:

$$\vec{\dot{m}}_m = -\frac{1}{24\mu}\left[\frac{1}{\overline{h^{-3}}} + \overline{h^3}\right]\nabla\bar{p} \qquad [7.19]$$

where the indicated averages are over areas local to the point under consideration. Equation (7.19) differs from (7.1) and this writer believes eq.(7.19) to be more accurate.

Equation (7.18) is actually valid for two-sided roughness, but has only been deduced for the case of no surface motion. Obviously, the subject of two-dimensional roughness requires further research.

VIII. Stokes Roughness

All analyses so far discussed have been for "Reynolds roughness" and have involved the assumption of the adequacy of Reynolds equation to describe the flow within the film. Now two conditions have to be met in order that Reynolds equation be a proper approximation to the Navier-Stokes equations. First, the film Reynolds number, $\rho U_m h/\mu$, must be small. Second, the change in film thickness per unit of film thickness must be small (i.e., $dh/dx \ll 1$). Whereas the first of these conditions is very often satisfied, the second condition may be violated by roughness contours, even when the slope of mean film-thickness is very small. In such instances, Stokes equations, not Reynolds, must be used.

In 1962, Citron (33) used Stokes equations to calculate the effects of longitudinal roughness in the gap between concentric rotating cylinders. But the effects of transverse roughness are more interesting. In an recent paper, *Sun & Chen* (34) have investigated transverse Stokes roughness effects on simple slider bearings. For this case, they write:

$$\frac{\partial u'}{\partial x'} + \frac{\partial v'}{\partial y'} = 0 \qquad\qquad [8.1]$$

$$\frac{\partial p'}{\partial x'} - \frac{\partial^2 u'}{\partial y'^2} = \epsilon^2 \, \frac{\partial^2 u'}{\partial x^2} \qquad\qquad [8.2]$$

$$\frac{\partial p'}{\partial y'} = \epsilon^2 \, \frac{\partial^2 v'}{\partial y'^2} + \epsilon^4 \, \frac{\partial^2 v'}{\partial x'^2} \qquad\qquad [8.3]$$

where:

$$u' = u/U \; ; \quad v' = v/\epsilon U \; ; \quad p = pc^2/\mu U L$$

$$x' = \frac{x}{L} \; ; \qquad y' = \frac{y}{c} \; ; \qquad \epsilon = c/L \qquad\qquad [8.4]$$

and the slider bearing in Fig. 4.1 will serve for nomenclature.

In the limit of small "ε", the terms on the rhs's of eqs. (8.2) and (8.3) disappear, and Reynolds relations are recovered. Sun & Chen solve these simpler relations subject to actual boundary conditions, including roughness, and insert the results into the rhs's to obtain improved solutions ("first iterations"). Figure 8.1 shows their results for load capacity of a flat slider bearing.
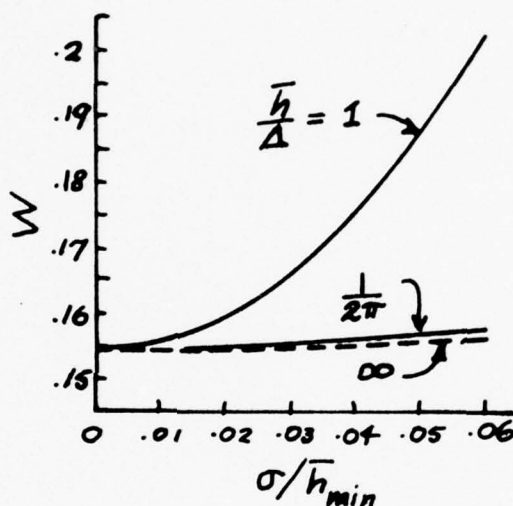
Figure 8.1 Load Capacity as Function of Random Roughness for Simple Slider ($\bar{h}_{max}/\bar{h}min=2\cdot7$) Stokes & Reynolds Roughness Theories Compared (from ref. 34).

The presentation in Fig. 8.1 is intended to reflect variations about an operating condition of $L\sim0$(25mm), $c\sim0$ (12.5μm), $\sigma\sim0(\cdot25$μm), and $\Delta\sim0$(12.5μm). Under these circumstances, Reynolds roughness theory predicts virtually no effect, whereas the authors' theory predicts as much as 30% load increase at $\sigma/c=0.06$ and a roughness wavelength equal

to the minimum film thickness (i.e., c/Δ=1)! On the other
hand, when c/Δ=1/2π, the predicted load increment only slight-
ly exceeds that obtained by Reynolds equation. The curves
are for typical random roughness.

In his doctoral dissertation, Rhow (28) studied the
effects of transverse and longitudinal rectangular grooving
by means of accurate numerical solutions of the biharmonic
Stokes equation.
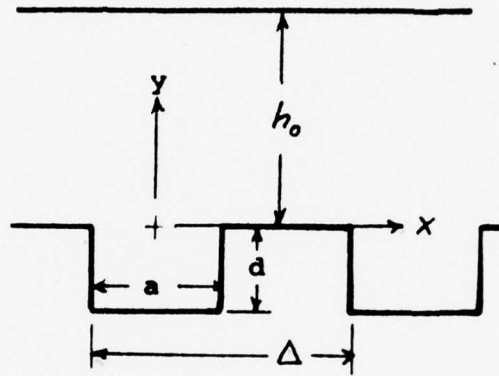
Figure 8.2   Nomenclature for Rectangular
Grooving.

This particular roughness configuration (see Fig. 8.2) was
chosen because of its simplicity for computer calculations,
its relevance to bearings with purposeful grooving, and its
indicative possibilities for other types of roughness. The
lineal flowrate corresponding to (a) $U \neq 0$, $\Delta p=0$ and (b) $U=0$,
$\Delta p \neq 0$ over one wavelength was calculated, and presented in the
following form (for transverse roughness):

$$\dot{m}_x = A\left[\frac{U}{2} \frac{\overline{h^{-2}}}{h^{-3}}\right] - B\left[\frac{1}{12\mu} \frac{1}{h^{-3}} \frac{\partial \bar{p}}{\partial x}\right] \qquad [8.5]$$

The coefficients "A" and "B" are unity for $\bar{h}/\Lambda \to \infty$ (Reynolds
roughness), and their deviation from unity is therefore a

measure of the importance of using Stokes equation.

Over wide ranges of geometric parameters (d/a, h_o/a, a/Δ) the coefficient "A" was found to lie fairly near unity, indicating that Reynolds roughness results for such flow will be reasonably accurate. On the other hand, as shown in Fig. (8.3) the Poiseuille coefficient "B" can drop substantially.
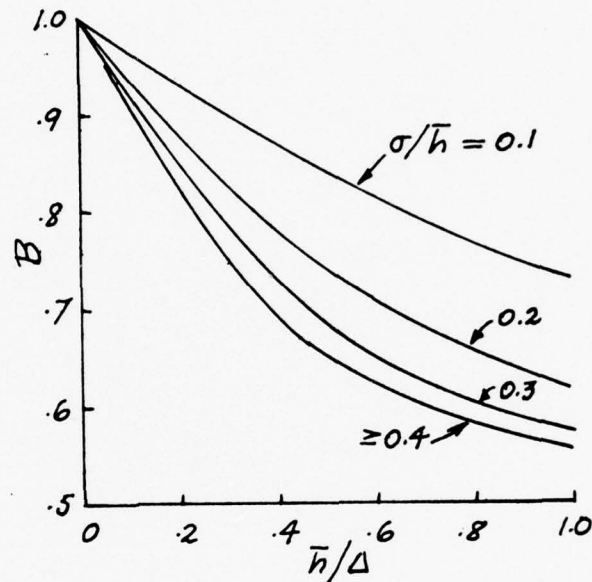
Figure 8.3   Poiseuille Coeff."B" for
Rectangular Grooving ($a=\Delta/2$)
(adapted from ref. 28).

To use the above results in a bearing calculation, one invokes the short-wavelength flux postulate, and uses local values of the film constructs A, B, $\overline{h^{-2}}$, $\overline{h^{-3}}$, etc., in eq. (8.5). This equation is then treated as a differential equation with $\dot{m}_x$ constant. Figure (8.4) shows Rhow's results[‡] for a flat slider. The difference between Stokes & Reynolds

----

[‡] For these calculations,"A" was taken as unity, and "B" was evaluated in a manner consistent with Fig. 8.3.

results is here much less than in the work of Sun & Chen (Fig.8.1).
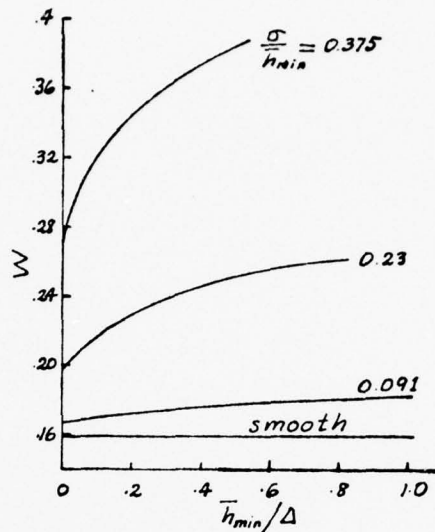
Figure 8.4   Load Capacity as Function of Roughness (rectangular grooving) for Simple Slider ($\bar{h}_{max}/\bar{h}_{min}=1$) Stokes Analysis (from ref. 28).

When reasonable allowances are made for differences in roughness configuration, bearing film convergence, etc., the differences in the results between Figs. 8.1 and 8.4 remain inexplicably large. Furthermore, the Sun-Chen conclusions tend to restrict drastically the applicability of Reynolds roughness theory. Accordingly, this writer has undertaken a different analysis which is less vulnerable to criticism than those previously made. The gist of this analysis, and its conclusion will here be presented.

Invoke the short-wavelength hypothesis, and consider two parallel plates, the upper one moving, the lower one rough, as in Figure 8.5. In Stokes approximation, the stream function satisfies the biharmonic equation.
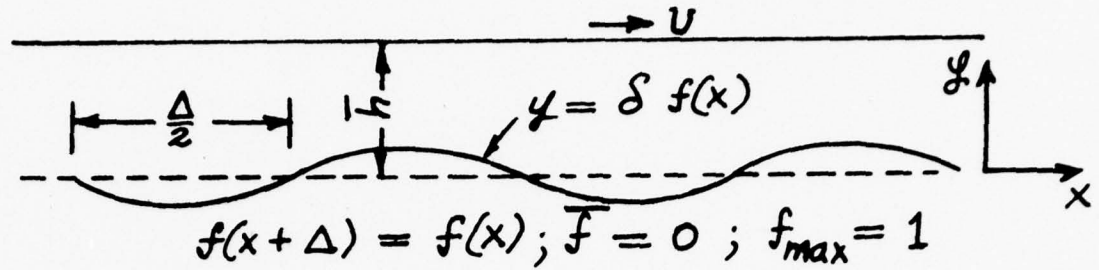
Figure 8.5.

Thus:

$$\nabla^4 \psi = 0 \qquad\qquad [8.6]$$

Both externally impressed shear and pressure gradient are accounted for by the following boundary conditions:

$$\left. \begin{array}{l} \psi(x,\epsilon f(x)) = \psi_y(x,\epsilon f(x)) = 0 \\[2ex] \psi_y(x,\bar{h}) = U \quad ; \quad \psi(x,\bar{h}) = \psi_H \end{array} \right\} \qquad [8.7]$$

An expansion is made in terms of amplitude, "δ", so that:

$$\psi = \psi_o(x,y) + \delta\psi_1(x,y) + \delta^2\psi_2(x,y) + \ldots\ldots \qquad [8.8]$$

With this expansion, there is always a "δ" small enough to accommodate any chosen roughness wavelength, Δ. The analysis must be carried through to second order, since first-order effects on load vanish.

It it both impossible and inappropriate to give details of the analysis here, but the conclusions can be summarized as follows:

In eq. (8.5): $A = 1-\delta^2\overline{f^2}(F^*-4)$ [8.9]

$$B = 1-3\delta^2\overline{f^2}(F^*-4)$$ [8.10]

where δ = (roughness amplitude)$/\bar{h}$

$f(x)$ = roughness shape function

expressed as = $\Sigma B_i \sin\omega_i x$ in Fourier Series.

$$F^* \equiv \frac{\overline{f(x)\Sigma\ F(h\omega_i)B_i\sin(\omega_i x)}^x}{\overline{f^2(x)}^x}$$ [8.11]

and: $F(\xi) = \dfrac{2\xi[\tanh\xi\{1+\xi\tanh\xi\}-\xi]}{(1+\xi^2)\tanh^2\xi-\xi^2}$ [8.12]

Equations (8.9-8.12) were used in eq. (8.5) for the slider bearing of Fig. 8.1, with $\sigma/\bar{h}_{min} = 0.06$, and with sinusoidal roughness.
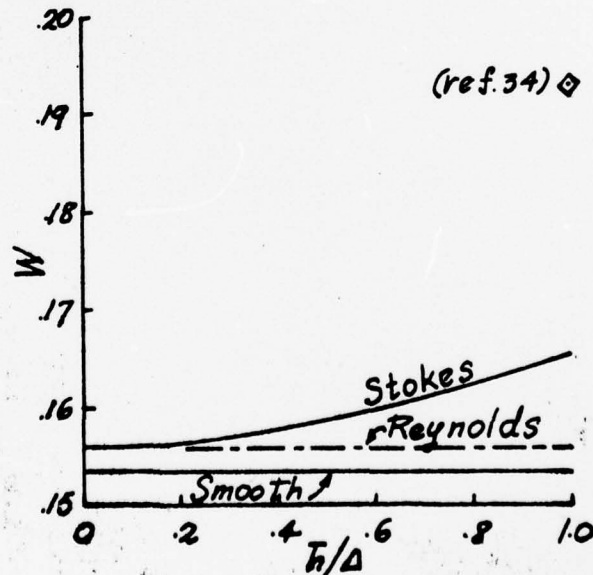
Figure 8.6   Load Capacity as Function of Sinusoidal Roughness for Simple Slider ($\bar{h}_{max}/\bar{h}_{min}=2\cdot7$) $\sigma/\bar{h}_{min}=0.06$.

The resulting curves are shown in Fig. 8.6. Again the pre-
dicted magnitude of the Stokes roughness effects differs
markedly from the corresponding prediction of Sun & Chen.
Since I am familiar with the ingredients of two independent
theories which conflict with the Sun-Chen results, I have
to conclude the Sun-Chen results are wrong. Why, I am not
certain, but possibly the iteration process they adopt does
not converge for $\Delta \sim \bar{h}$. For example, in general:

$$\frac{\partial^2 u'}{\partial x'^2} = 0 \left(\frac{L}{\Delta}\right)^2$$

so that in eq. (8.2), $\varepsilon \frac{\partial^2 u'}{\partial x'^2} = 0 \left(\frac{\bar{h}}{\Delta}\right)^2$

Thus the rhs of (8.2) is not small compared with the lhs
when $\bar{h}/\Delta \equiv 1$. No doubt, with this questioning of their results,
the authors will recheck their work and we shall hear more
of the matter.

IX. Molecular Slip

There are occasions when it is pointless to consider roughness effects without simultaneously considering molecular slip effects. For example, the "flying heads" used for information retrieval from rotating disks in modern computers are actually small air slider bearings. Minimum mean clearance in these devices is now being reduced to approximately 0.4μm. At the same time, the mean-free path of the air molecules is about 0.1μm and the roughness amplitude of the surface finish is about 0.03μm.

The first effects of rarefaction are customarily accounted for by the use of slip-flow aerodynamics. Thus, within the flow interior, standard continuum-fluid differential equations are employed, while failure of the macroscopic fluid velocity to agree with that of its bounding surfaces is modelled by the Maxwell slip condition. Thus:

$$\Delta u = \lambda \frac{\partial u}{\partial n} \qquad\qquad [9.1]$$

Here "Δu" is the above-mentioned tangential velocity discrepancy, "λ" is the mean-free molecular path, and "$\partial u/\partial n$" is the velocity derivative normal to the surface. When eq. (9.1) is used in connection with Reynolds equation (Burgdorfer, 1959,[‡]) the lineal mass flow is given by the following simple equation:

$$\dot{m}_x = \rho \frac{Uh}{2} - \frac{h^3}{12\mu}\left(1 + \frac{6\lambda}{h}\right) \frac{\partial p}{\partial x} \qquad\qquad [9.2]$$

In the presence of one-sided roughness, smoothening by means of the flux continuity postulate and the load in-

---

[‡] Trans. A.S.M.E., 80, (1959), p.94

compressibity assumption[*] yields, for transverse roughness:

$$\frac{12\mu RTL\dot{m}_x}{p_a^2 c^3} = \Lambda_x \left(\frac{\tilde{H}^{-2}}{\tilde{H}^{-3}}\right)\pi_o - \frac{1}{\tilde{H}^{-3}}\pi_o \frac{\partial \pi_o}{\partial \xi} \tag{9.3}$$

where:

$$\tilde{H}^{-2} \equiv \overline{[H^2 + 6\frac{\lambda_a}{c}\frac{H}{\pi_o}]^{-1}}$$

$$\tilde{H}^{-3} \equiv \overline{[H^3 + 6\frac{\lambda_a}{c}\frac{H^2}{\pi_o}]^{-1}} \left. \right\} \tag{9.4}$$

Correspondingly, for longitudinal roughness, one gets:

$$\frac{12\mu RTL}{p_a^2 c^3}\dot{m}_y = \Lambda_y \bar{H}\pi_o - \tilde{H}^3 \pi_o\frac{\partial \pi_o}{\partial \eta} \tag{9.5}$$

where: $\tilde{H}^3 \equiv \overline{(H^3 + 6\frac{\lambda_a}{c}\frac{H^2}{\pi_o})}$ \qquad (9.6)

The components can be combined, as in eq. (6.8), to form the lineal mass flux vector.

Now the foregoing analysis breaks down for short roughness wavelengths. Recently Chang and this author have performed kinetic-theory calculations for rectangular grooving. In this work the Boltzmann equation is solved by dividing velocity space into four iso-energetic groups of different direction. The method is suitable for low macroscopic speeds, and, in appropriate limits, yields accurate slip flow or continuum results. Virtually complete overlap with the continuum work of Rhow and Elrod is obtained. It is

---

[*] Both are endorsed by an unpublished multiple-scale treatment of the author.

hoped that details will be published, but the gist of the principal conclusion can be stated as follow:

"When the effects of molecular slip and of one-sided, trans-verse Stokes roughness are simultaneously present, one can use eg. (9.3), modified by the same continuum correction factors as would be used with eq.(8.5) for the same roughness contour"

X. Conclusions and Acknowledgment

Although the accomplishments of analysis in predicting the effects of roughness on laminar lubricating films are perhaps encouraging, the work is incomplete, and a number of differences in outlook and results remain to be reconciled.

Two-sided Reynolds roughness has been analyzed only for parallel striations on opposing surfaces. Two-dimensional (i.e., non-striated), roughness has been treated only for stationary surfaces. Even the first effects of Stokes roughness are in some dispute, though there is agreement that Reynolds equation is not as suitable as we might like for roughness analyses, due to its long-wavelength restriction. Much of the more recent work would benefit from a less heuristic development. And finally, the areas for utility of statistical analyses need to be better delineated.

NOMENCLATURE
_____

(Some symbols which are used in a restricted portion of the text are defined there on-the-spot).

A   correction coefficient in Reynolds eq., eq.8.5

B   correction coefficient in Reynolds eq., eq.8.5

c   nominal clearance of bearing (= min. cl. for sliders) parameter in roughness distribution, eq.4.7

C C_f, friction force/load

h   film thickness, including roughness $\bar{h}$, mean local film thickness. $h = \bar{h}+\theta$; h_s = specific value of θ

H   h/c

L   characteristic gross dimension of bearing

m   slope of slider bearing $(h_{max}-h_{min})/L$
    $\dot{m}$, lineal mass flow rate per unit transverse distance

n   coordinate perpendicular to striations
    Also, number of waves used in deterministic calculations

p   fluid pressure

Q   lineal volumetric flow in film.   Volume per unit time per unit distance transverse to flow

r   distance from asperity center

R R_o asperity radius

s   coordinate parallel to striations

t   time

u   fluid velocity, x-direction

U   surface velocity in x-direction

v   fluid velocity, y-direction

W $(load)c^2/\mu UL^2$

x   cartesian coordinate

y   cartesian coordinate

z   coordinate perpendicular to striations. See Fig. 1.1

β orientation angle of striations. See Fig. 1.1

δ roughness amplitude/mean film thickness

Δ striation wavelength

ε Δ/L or c/L

ζ z/Δ

η y/L also, fluid viscosity

θ circumferential angle, or magnitude of roughness

λ mean-free path of molecules; λ_a = ambient λ

Λ $6\mu UL/P_a c^2$; for liquids, use $p_a = \rho \left(\frac{\partial p}{\partial \rho}\right)_T$

μ fluid viscosity

π p/p_a

σ standard deviation of roughness

τ $p_a c^2 t/12\mu L^2$; for liquids, use $p_a = \rho \left(\frac{\partial p}{\partial \rho}\right)_T$

ψ stream function. $\partial\psi/\partial y = u$; $\partial\psi/\partial x = -v$

Special Symbols & Subscripts

m   ----- mean or local space average

$\overline{(\ )}$ ----- mean, statistical or space average

< >   expected value, or statistical mean

subscript zeroth order, first order, etc. function of an

0,1,2,   expansion, or used to signify location.

a   ambient

$\hat{n}$ unit normal in n-direction

$\hat{j}$ unit normal in s-direction

BIBLIOGRAPHY

1   Michell, A.G.M., "Lubrication. Its Principles and Prac-
    tice", Blackie & Son, Ltd., 1950, Appendix I.

2   Salama, M.E., "The Effect of Macro-Roughness on the Per-
    formance of Parallel Thrust Bearings", Proc. Inst. Mech.
    Engrs., 1950, Vol. 162, p. 149.

3   Cameron, A., "Theory of Rough Pads", Pametrada Report
    No. 92, 1951.

4   Burton, R.A., "Effects of Two-Dimensional, Sinusoidal
    Roughness on the Load Support Characteristics of a Lu-
    bricant Film", Journal of Basic Engrg., Trans. A.S.M.E.,
    Series D, Vol. 84, June 1963, pp. 258-64.

5   Davies, M.G., "The Generation of Pressure between Rough
    Fluid-Lubricated, Moving Deformable Surfaces", Lubrica-
    tion Engineering, June 1963, p. 246.

6   Tipei, N. & Pascal H., "Micro- and Macrogeometry Effect
    on Pressures in Three-Dimensinal Lubrication", Review
    of the Roumanian Science Technology, Mec. Appl., Vol.11,
    No. 3, 1966, p. 699.

7   Dowson, D. & Whomes, T.L., "The Effect of Surface Rough-
    ness upon the Lubrication of Rigid Cylindrical Rollers
    ------I. Theoretical", Wear, Vol 18, 1971, pp. 129-150.

8   Shelly, P. & Ettles, C., "Effect of Transverse and Lon-
    gitudinal Surface Waviness on the Operation of Journal
    Bearings", Jnl. Mech. Engrg. Sci., Vol. 14, No.3, 1972,
    pp. 168-172.

9   Tønder, K. & Christensen, H., "Lubrication of Cylindri-
    cal Rollers with Surface Corrugations", Wear, Vol. 20,
    1972, pp. 309-314.

10 Muijderman, E.A., "Spiral Groove Bearings", Philips
    Technical Library, 1966.

11a Boeker, G.F. (U.S. Classified Document) circa 1944.

11b Whipple, R.T.P., "Herringbone Pattern Thrust Bearings",
    A.E.R.E. T/M 29, 1949.

12 Hirs, G.G., "Externally Pressurized Bearings with Inher-
    ent Friction Compensation", Journal of Applied Mechanics,
    Trans. A.S.M.E., Paper No. 65- APM-B.

13   Elrod, H.G., "A Generalized Narrow-Groove Theory for the
      Gas-Lubricated Herringbone Thrust Bearing", Paper 18,
      4th Biannual Gas Bearing Symposium, Univ. of Southamp-
      ton, England, 22-25 April 1969, Vol. 3 of Proceedings.

14   Vohr, J.H. & Pan, C.H.T., "On the Spiral-Grooved Self-
      Acting Gas Bearing", Mechanical Technology, Inc.,
      Latham, N.Y., U.S.A., M.T.I. Tech. Rpt. MT 16352, pre-
      pared under ONR Contr. Nonr-373(00), Task NR 061-031,
      (1963).

15   Elrod, H.G., "Thin-Film Lubrication Theory for Newtonian
      Fluids with Surfaces Possessing Striated Roughness or
      Grooving", Journal of Lubrication Technology, Series F
      of Trans. A.S.M.E., Oct. 1973, pp. 484-489.

16   Tzeng, S.T. & Saibel, E., "Surface Roughness Effect on
      Slider Lubrication", ASLE Transactions, Vol. 10,(1967),
      pp. 334-38.

17   Tzeng, S.T. & Saibel, E., "On the Effects of Surface
      Roughness in the Hydrodynamic Lubrication Theory of a
      Short Journal Bearing", Wear, Vol. 10, (1967), pp.
      179-184.

18   Christensen, H., "Stochastic Models for Hydrodynamic
      Lubrication of Rough Surfaces", Proc. Instn. Mech.
      Engrs., Vol. 184, Pt.1, No. 55, (1969-70), pp. 1013-22.

19   Christensen, H. and Tønder, K., "The Hydrodynamic Lubri-
      cation of Rough Bearing Surfaces of Finite Width",
      Journal of Lubrication Technology, Trans. A.S.M.E.,
      July 1971, pp.324-330.

20   Christensen, H. and Tønder, K., "The Hydrodynamic Lubri-
      cation of Rough Journal Bearings", Journal of Lubrica-
      tion Technology, Trans. A.S.M.E., April 1973, pp.166-172.

21   Elrod, H.G., "A Generalized Narrow Groove Theory Includ-
      ing Ambient Edge Corrections", 5th Bi Annual Gas Bearing
      Symposium, Univ. of Southampton,England, (1974).

22   Gupta, P.K. Coleman, R.L. & Pan, C.H.T., "Ambient Edge
      Correction for the Locally Incompressible Narrow-Groove
      Theory", Journal of Lubrication Technology, Trans. A.S.M.
      E., Series F., Vol. 96, No. 2, (Apr. 1974), pp. 284-290.

23   Berthe, D. & Godet, Maurice, "Equation de l'écoulement
      laminaire entre deux parois rapprochées en mouvement
      relatif", C.R.Acad. Sc. Paris, Series A, t.272 (14.avril
      1971), pp. 1010-1013.

24   Michau, B., Lafont, F., Berthe, D. and Godet, M.,
      "Influence de la modulation de la pression hertzienne á
      l'intérieur d'un contact", Revue du GAMI, Oct. 1973.

25   Tallian, T.E., "Pressure and Traction Rippling in Elasto-
      hydrodynamic Contact of Rough Surfaces", Journal of
      Lubrication Technology, Trans. A.S.M.E., Series F, Vol.
      96, July 1974, pp. 398-409.

26   Chow, L.S.H. & Cheng, H.S., "The Effect of Surface Rough-
      ness on the Average Film Thickness between Lubricated
      Rollers", Journal of Lubrication Technology, Trans.
      A.S.M.E., Vol. 98, Series F, (Jan. 1976), pp. 117-124.

27   Rhow, S.K. and Elrod, H.G., "The Effects on Bearing Load-
      Carrying Capacity of Two-Sided Striated Roughness", Jour-
      nal of Lubrication Technology, Trans. A.S.M.E., Series F,
      Vol. 96, No. 4, (Oct. 1974), pp. 554-560 & 640.

28   Rhow, S.K. and Elrod, H.G., "Effects of Surface Roughness
      or Grooving on Thin, Laminar Lubricating Films", Rpt.
      23, Lubrication Research Lab., Department of Mechnical
      and Nuclear Engineering, Columbia Univ., New York, N.Y.
      10027.

29   Hamilton, D.B., Walowit, J.A. & Allen, C.M., "A Theory
      of Lubrication by Micro-Irregularities", Journal of
      Basic Engineering, Trans. A.S.M.E., (Mar. 1966), pp.
      177-185.

30   Tsao, Y.H. & Tong, K.N., "A Model for Mixed Lubrication",
      Trans. A.S.L.E., Vol. 18, No. 2, pp. 90-96.

31   Elrod, H.G., "Two Simple Theorems for Establishing
      Bounds on the Total Heat Flow in Steady-State Heat-
      Conduction Problems with Convective Boundary Conditions",
      Journal of Heat Transfer, Trans. A.S.M.E., (Feb. 1974),
      pp. 65-70.

32   Private Communication from Prof. M.M. Yovanovich, Univ.
      of Waterloo, Waterloo, Ontario, Canada.

33   Citron, S.J., "Slow Viscous Flow between Rotating Con-
      centric Infinite Cylinders with Axial Roughness", Jour-
      nal of Applied Mechanics, Trans. A.S.M.E., Vol. 84,
      (1962), pp. 188-92.

34   Sun, D.C. & Chen, K.K., "First Effects of Stokes Rough-
      ness on Hydrodynamic Lubrication", Journal of Lubrica-
      tion Technology, Trans. A.S.M.E., Series F, Vol. 99,
      (Jan. 1977), pp. 2-9.

DISTRIBUTION LIST

Mr. Wilbur Shapiro
Manager
Friction & Lubrication
   Laboratory

The Franklin Institute
   Research Laboratories
The Benjamin Franklin Pw.
Philadelphia, PA 19103

Mr. Arthur Huxley
Admiralty Compass
   Observatory
Ditton Park
Slough, Bucks, England

Office of Naval Research
Code 438
800 N. Quincy Street
Arlington, VA 22217

Code 2627
Naval Research Laboratory
Washington, D.C. 20375

Mr. J. Dray
Code 6148
Naval Ship Engineering
   Center
Washington, D.C. 20362

R. K. Brodersen
Martin Marietta Aerospace
Orlando Division
P. O. Box 5837   MP 326
Orlando, Florida 32805

J. B. Huff, Director
Guidance & Control Dir.
Missile Command Lab.
DARCOM-RG
Redstone Arsenal, AL 35809

Dr. A. Eshel
Ampex Corporation
401 Broadway
Redwood City, CA 94063

Technical Library
Naval Ocean Systems Center
San Diego, CA 92132

Mr. Steve Rohrbough
Honeywell Inc.
Aerospace Division
13350 U.S. Highway 19
St. Petersburg, FL 33733

Office of Naval Research
Code 473
800 N. Quincy Street
Arlington, VA 22217

Library (Code 09GS)
Naval Sea Systems
      Command
Washington,D.C. 20362

Library (Code 5641)
David W. Taylor Naval Ship
   Research & Development
   Center
Bethesda, MD 20084

Air Force Office of
   Scientific Research/NA
Building 410
Bolling AFB
Washington, D.C. 20332

Mr. R. Dayton (APFL)
AF Aero Propulsion Lab.
Wright-Patterson AFB
OH 45433

Army Research Office
P. O. Box 12211
Research Triangle Park
   N.C. 27709

Librarian
Naval Surface Weapons
White Oak Laboratory
Silver Spring, MD 2091

Prof. R. Di Prima
Dept. of Mathematics
Rensselaer Polytechnic
   Institute
Troy, New York 12181

Office of Naval Resear
Code 1021P (ONRL)
800 N. Quincy Street
Arlington, VA 22217

Code 6034
Naval Ship Engineering
      Center
Washington, D.C. 20362

Strategic Systems Proj
   Office (SP230)
Department of the Navy
Washington, D.C. 20376

Mr. W. M. Crim
Office of Coal Researcl
Energy Research &
   Development Administ.
Washington, D.C. 20545

Defense Documentation
Center
Cameron Station
Alexandria, VA 22314

Library
Naval Academy
Annapolis, MD 21402

Dr. A. Wood
Office of Naval Research
Branch Office
495 Summer Street
Boston, MA 02210

Library
C. S. Draper Laboratory
555 Technology Square
Cambridge, MA 02139

Director
Office of Naval Research
Branch Office
536 South Clark Street
Chicago, IL 60605

Mr. P. H. Broussard, Jr.
Guidance and Control
Division
National Aeronautics &

Space Administration
George C. Marshall Space
Flight Center
Huntsville, AL 35812

Prof. D. D. Fuller
Department of
Mechanical Engineering
Columbia University
New York, N.Y. 10027

Mr. Anthony W. Lawrence
Northrop Corporation
Electronics Division
100 Morse Street
Norwood, MA 02062

Mr. Stanley L. Zedekar
Dept. 244-2, Bldg. 71
Autonetics
P. O. Box 4181
Anaheim, CA 92803

Dr. Coda Pan
Shaker Research Corp.
Northway 10 Executive Pk.
Ballston Lake, NY 12019

Commanding Officer
NROTC Naval Administrative
Unit
Massachusetts Institute
of Technology

Cambridge, MA 02139

Mr. W. J. Anderson
NASA Lewis Research Ct.
Cleveland, OH 44871

Prof. William K. Stair
Assistant Dean, Mechanical
& Aerospace Engineering
University of Tennessee
Knoxville, TN 37916

Mr. K. Liebler, Supervisor
Head & Media Development
Control Data Corporation
Normandale Division

7801 Computer Avenue
Minneapolis, MN 55424

Director
Office of Naval Research
Branch Office
1030 E. Green Street
Pasadena, CA 91101

Technical Library
David W. Taylor Naval
Ship Research & Dev.
Annapolis Laboratory
Annapolis, MD 21402

NASA Scientific & Tech
Information Facility
P. O. Box 8757
Baltimore/Washington
International Airpor

Maryland 21240

Dr. Edgar J. Gunter, J
University of Virginia
School of Engineering
& Applied Science
Charlottesville, VA 22

Prof. Ralph Burton
Dept. of Mechanical En
& Astronautical Sci.
Northwestern Universit
Evanston, IL 60210

Mr. Otto Decker
Mechanical Tech., Inc.
968 Albany-Shaker Road
Latham, NY 12110

Library
Naval Postgraduate Sch
Monterey, CA 93940

Prof. V. Castelli
Department of
Mechanical Engineeru
Columbia University
New York, N.Y. 10027

Technical Library
Naval Ship Engrg. Cent
Philadelphia Division
Philadelphia, PA 19112

DOCUMENT CONTROL DATA - R&D

(Security classification of title, body of abstract and indexing annotation must be entered when the overall report is classified)

1. ORIGINATING ACTIVITY (Corporate author)	2a. REPORT SECURITY CLASSIFICATION
Columbia University, Department of Mechanical and Nuclear Engineering, Lubrication Research Laboratory	Unclassified
	2b. GROUP

3. REPORT TITLE

A Review of Theories for the Fluid Dynamic Effects of Roughness on Laminar Lubricating Films.

4. DESCRIPTIVE NOTES *(Type of report and inclusive dates)*

Technical Report.

5. AUTHOR(S) *(Last name, first name, initial)*

Harold G. Elrod   58p.

6. REPORT DATE	7a. TOTAL NO. OF PAGES	7b. NO. OF REFS
December 1977	52	34

8a. CONTRACT OR GRANT NO.	9a. ORIGINATOR'S REPORT NUMBER(S)
N00014-76-C-0105	No. 27 Lubrication Research Lab
b. PROJECT NO.	
c. Task NR 062-360	9b. OTHER REPORT NO(S) (Any other numbers that may be assigned this report)
d.	

10. AVAILABILITY/LIMITATION NOTICES

This document has been approved for public release and sale; its distribution is unlimited.

11. SUPPLEMENTARY NOTES	12. SPONSORING MILITARY ACTIVITY
	Office of Naval Research

13. ABSTRACT

This report contains a comprehensive survey of theoretical work on the fluid dynamic effects of roughness in lubrication.

Of necessity, much of the report deals with Reynolds roughness; that is, roughness which can be locally analyzed with Reynolds equation because the wavelength of the roughness is not too short. One-sided and two-sided striated roughnesses are considered. Statistical and multiple-scale treatments are discussed and intercompared. Finally, the effects of short-wavelength roughness (Stokes roughness) are treated, as well as the consequences of slip in highly rarefied situations.

Some new results for isotropic Reynolds roughness, for Stokes roughness, and for molecular slip are given preliminary exposure.

DD FORM 1473
1 JAN 64

088 945

LB

14. KEY WORDS	LINK A		LINK B		LINK C	
	ROLE	WT	ROLE	WT	ROLE	WT
Surface roughness Reynolds Equation						

INSTRUCTIONS

1. ORIGINATING ACTIVITY: Enter the name and address of the contractor, subcontractor, grantee, Department of Defense activity or other organization (corporate author) issuing the report.

2a. REPORT SECURITY CLASSIFICATION: Enter the overall security classification of the report. Indicate whether "Restricted Data" is included. Marking is to be in accordance with appropriate security regulations.

2b. GROUP: Automatic downgrading is specified in DoD Directive 5200.10 and Armed Forces Industrial Manual. Enter the group number. Also, when applicable, show that optional markings have been used for Group 3 and Group 4 as authorized.

3. REPORT TITLE: Enter the complete report title in all capital letters. Titles in all cases should be unclassified. If a meaningful title cannot be selected without classification, show title classification in all capitals in parenthesis immediately following the title.

4. DESCRIPTIVE NOTES: If appropriate, enter the type of report, e.g., interim, progress, summary, annual, or final. Give the inclusive dates when a specific reporting period is covered.

5. AUTHOR(S): Enter the name(s) of author(s) as shown on or in the report. Enter last name, first name, middle initial. If military, show rank and branch of service. The name of the principal author is an absolute minimum requirement.

6. REPORT DATE: Enter the date of the report as day, month, year; or month, year. If more than one date appears on the report, use date of publication.

7a. TOTAL NUMBER OF PAGES: The total page count should follow normal pagination procedures, i.e., enter the number of pages containing information.

7b. NUMBER OF REFERENCES: Enter the total number of references cited in the report.

8a. CONTRACT OR GRANT NUMBER: If appropriate, enter the applicable number of the contract or grant under which the report was written.

8b, 8c, & 8d. PROJECT NUMBER: Enter the appropriate military department identification, such as project number, subproject number, system numbers, task number, etc.

9a. ORIGINATOR'S REPORT NUMBER(S): Enter the official report number by which the document will be identified and controlled by the originating activity. This number must be unique to this report.

9b. OTHER REPORT NUMBER(S): If the report has been assigned any other report numbers (either by the originator or by the sponsor), also enter this number(s).

10. AVAILABILITY/LIMITATION NOTICES: Enter any limitations on further dissemination of the report, other than those imposed by security classification, using standard statements such as:

   (1) "Qualified requesters may obtain copies of this report from DDC."

   (2) "Foreign announcement and dissemination of this report by DDC is not authorized."

   (3) "U. S. Government agencies may obtain copies of this report directly from DDC. Other qualified DDC users shall request through

   _____ ."

   (4) "U. S. military agencies may obtain copies of this report directly from DDC. Other qualified users shall request through

   _____ ."

   (5) "All distribution of this report is controlled. Qualified DDC users shall request through

   _____ ."

   If the report has been furnished to the Office of Technical Services, Department of Commerce, for sale to the public, indicate this fact and enter the price, if known.

11. SUPPLEMENTARY NOTES: Use for additional explanatory notes.

12. SPONSORING MILITARY ACTIVITY: Enter the name of the departmental project office or laboratory sponsoring (paying for) the research and development. Include address.

13. ABSTRACT: Enter an abstract giving a brief and factual summary of the document indicative of the report, even though it may also appear elsewhere in the body of the technical report. If additional space is required, a continuation sheet shall be attached.

   It is highly desirable that the abstract of classified reports be unclassified. Each paragraph of the abstract shall end with an indication of the military security classification of the information in the paragraph, represented as (TS), (S), (C), or (U).

   There is no limitation on the length of the abstract. However, the suggested length is from 150 to 225 words.

14. KEY WORDS: Key words are technically meaningful terms or short phrases that characterize a report and may be used as index entries for cataloging the report. Key words must be selected so that no security classification is required. Identifiers, such as equipment model designation, trade name, military project code name, geographic location, may be used as key words but will be followed by an indication of technical context. The assignment of links, roles, and weights is optional.

DD FORM 1 JAN 64 1473 (BACK)